CFD Prediction of Heat Transfer to a Steel Beam under Ceiling

TAKASHI WAKAMATSU
Institute of Construction Technology, Kumagai Gumi Co
Onigakubo 1043, Tsukuba, Ibaraki, Japan

YUJI HASEMI
Department of Architecture and Architectural Engineering School of Science and Engineering
Waseda University
3-4-1 Ookubo, Shinjuku, Tokyo, Japan

ALEXANDER. V. PTCHELINTSEV
VTT Building Technology
Kivimiehentie 4, Espoo, P.O.Box 1803, fin-02044 VTT, Finland

YOSHIHIKO HAYASHI
Building Research Institute, Ministry of Construction
Tatehara 1, Tukuba-City, Ibaraki-Pref.

ABSTRACT

A prediction of the thermal response of a steel beam installed beneath a ceiling and exposed to a localized fire source was performed by using CFD model. The validity of steady state calculation has been verified by results of experiments. Concerning the heat flux, the difference between analytical results and experimental values increases with increasing dimensionless heat release rate $Q^*_{DH_B} \equiv Q/\rho C_P T_0 g^{1/2} DH_B{}^{3/2}$. In the case of the lower flange, the difference between the analytical result and experimental value increases rapidly over the range of Q^*_{DHB} from 0.35 to 0.5, reaching the maximum value of about 22 (kW/m^2). This difference is equivalent to 56% of the maximum heat flux in the experiment. While the error for the heat flux scattered within 20% to 56% of the maximum heat flux measured in the experiment, the maximum error for the temperature remained 22%.

KEYWORDS: localized fire ,CFD model, compressible ,prediction ,thermal response , steel beam

INTORODUCTION

In Japan ,fire resistance tests for building components generally evaluate with the temperature assuming exposure of the component to a fully developed fire by the Building Standards. Given a sufficiently wide space in a building or a sufficiently wide opening for the space comparing with the fire load ,for example atriums ,airport, parking buildings etc. any fire would be of fuel-controlled type and the effect of heating on structural members could be localized. It may be assumed that the rise in temperature is smaller than in the event of all the members being subject to heating by fire. When a metal structural member is heated only locally in a fire , the temperature of the member will be uniformed rapidly due to the accelerated heat conduction through the member itself. This is due to the thermal conductivity of metal being much higher than that of other construction materials. In such circumstances ,the localized temperature rise may be restricted. In the case where a load bearing member is heated only locally in fire ,if a new method is established which can accurately predict the thermal response of the components , the fire safety design will become more rational. Now, the authors have assumed a typical case of localized fire, in which the H-section steel beam installed beneath the ceiling and exposed to localized heating with a heat source on the floor, and heating characteristics of the member were measured through experiment[1]. Subsequently, we have formulated heat flux distribution on every part of the beam as a function of heat release rate and the distance from the fire source to the member. Then we made a FEM and F.D.M-based numerical calculation of temperature responses, and these numerical models were verified for its validity by comparing the numerical results of temperature with those obtained through the experiment [2),3)].

The concept of applying CFD model developed in the field of fluid dynamics to study of fire safety science has existed since early times. However, it faces many problems to ensure practical accuracy for the analysis. Most of these problems are attributed to the fact that fire is a complicated physical phenomenon involving combustion. A calculation model which can treat properly the effects of combustion and radiation, if available, would help development promising methods. Recently, Yoshie et al conducted a fundamental study, based on the field model, to compare analytical results and an experimental formula concerning the speed and temperature of thermal plume from the heat source [4),5),6)]. The results of this study showed that the model was able to predict the flow field of this thermal plume with practical accuracy. Temperature prediction of members according to F.E.M. and F.D.M described above required the heat flux as a boundary condition[2),3)].The heat flux data were obtained through time-consuming, expensive experiments. At present, facilities and professionals for such experiments are limited. Accordingly, if the heat flux itself can be calculated not through experiments, but through simulations, it will not be necessary to perform experiments each time the shapes, etc., of members change.

In view of the above mentioned point , this paper studied the appropriateness of the analytical method of heating conditions (heat flux and temperature) of members exposed to localized fire using the field model. The final purpose of this study is to predict the heating condition of the members by means of calculation only, without experiments.

OUTLINE OF SOFIE

SOFIE (Simulation Of Fires In Enclosures) is used as a calculation code[7)]. SOFIE is a field model for the prediction of fires in compartments. The SOFIE code aims to reproduce the core features of current commercially-available, general-purpose CFD codes.

SOFIE developed mainly by Cranfield University of England, Lund University of Sweden, VTT of Finland, and CSTB of France. The results of experiment which assumed room fire and analytical results using this model agreed well [8)].

The governing equations of approximative compressible flow which assume steady pressure

field is used in SOFIE , and SOFIE has the following principal features:

- Eddy break-up combustion model
- Three-dimensional finite volume method
- κ - ε turbulence model with buoyancy modifications

In addition to the above, this program has thermal characteristics of several representative materials stored as data files and can use them considering temperature-dependency.

NUMERICAL SIMULATION

Analysis is made of a heat transfer field in which an H shaped steel beam is located under a ceiling, and the center of the beam is heated by a fire source on the floor. For this analysis, considering its symmetrical form of the specimen, we prepared a 1/4 three dimensional thermal analysis model representing the ceiling and beam. FIGURE.1 shows an analytical model. An actual fire source used in the experiment was a 0.5(m)diameter round porous burner. Since a rectangular coordinate system was used in this calculation , the portion shown in the figure was used as a inflow boundary surface so that the area was equivalent to 1/4 of the round burner area. For calculation, a solution domain of 2.1 (x)$\times$3.0 (y)$\times$2.3 (z)(m) was divided into a total of 14535 grid cells, each being 19$\times$17$\times$45. As boundary conditions, the whole of the top surface at a height of 1(m)in the y direction from the ceiling slab was defined as a static-pressure boundary. The vertical side-wall which runs parallel to the beam axis was also defined as a static-pressure boundary, whilst the axial end wall was defined as a solid. The pressure boundaries/walls were located at a (horizontal) distance of one (m) from the edge of the perlite ceiling slab. The grid cells shown in FIGURE.1 are portion used to define the wall as a boundary condition. As shown in FIGURE. 2, the vertical section of the H-shaped beam member was represented using six cells vertically and two horizontally. Since a minimum of two cells must be used in any direction when a solid is defined, the web and flange were divided into two cells in a vertical direction. Since a uniform grid spacing was assumed, this gives a mesh which is a poor match to the true geometry, but this was inevitable due to the relatively narrow steel thickness compared to the overall dimensions of the test rig.

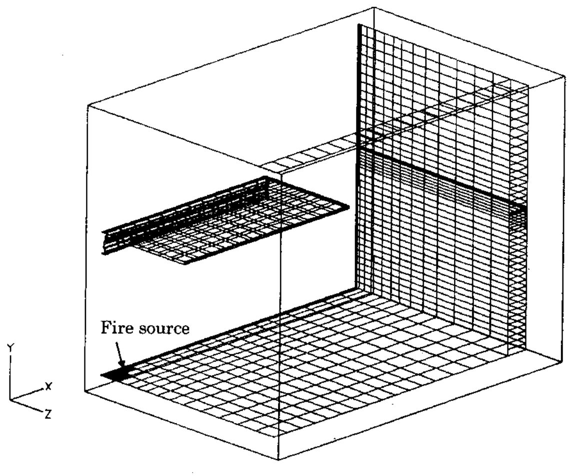

FIGURE. 1 Computational mesh

OUTLINE OF CALCULATION

For this study, SOFIE(ver-s20701,standard k-ε turbulence model) was employed with buoyancy modifications, and with optional Rodi center-line corrections[9]. The eddy break-up sub-model was applied for combustion, with propane being taken as the fuel. The pressure correction algorithm SIMPLEC scheme is used together with momentum interpolation for pressure smoothing in the non-staggered grid. The non-staggered grid defines various quantities at the same point in the control volume.

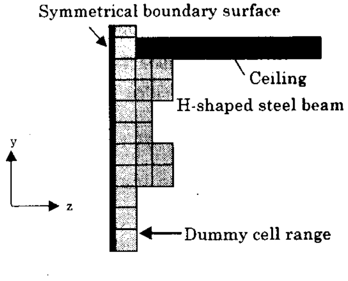

FIGURE. 2 Division of beam member into

Thermal radiation is computed using a deterministic ray-tracing approach DTRM[10]based upon the discrete transfer algorithm. 'Weighted sum of grey gas' WSGG solutions[11] to the radiation transfer equation are available, together with a fully-coupled soot-radiation model. The CGSTAB conjugate-gradient solver was used for the pressure correction equation in all cases. The HYBRID interpolation scheme was used for all solved variables except velocities, for which the SOUP (Second-Order UPwind) scheme was chosen[12].

The ordinary steel was defined for beam, perlite for the ceiling slab, and the high-density concrete for the floor . The properties for the steel and perlite were derived from experimental measurements and expressed as 4th-order polynomials of temperature as follows:

$$C_{p,steel} = 582.3 - 889.6t + 2289t^2 - 1486t^3 + 297t^4 \quad \cdots (1)$$

$$C_{p,perlite} = 1493 - 4658t + 13743t^2 - 14585t^3 + 5128t^4 \quad \cdots (2)$$

$$\kappa_{steel} = 70.45 - 27.67t - 48.47t^2 + 47.22t^3 - 10.68t^4 \quad \cdots (3)$$

$$\kappa_{perlite} = 0.3314 - 0.8834t + 1.932t^2 - 1.960t^3 + 0.7226t^4 \quad \cdots (4)$$

where; $t = T/1000$

The material densities were assumed to be as follows: 7850 kg/m^3 constant for steel, 789 kg/m^3 constant for perlite, 2800 kg/m^3 constant for high-density concrete. The emissivity of all solid surfaces was assumed to be 0.9 . The inflow boundary conditions were set as κ =0.005, ε =0.001 m^2/s^3 referred to S.Welch and A. Ptchelintsev's research [13] in which the thermal response of a steel beam exposed to localized fire was analyzed. Minimum residual (mass error)was set to 10^{-5}, and the external air temperature was set to 290 (k). The time for the calculation was about 900 seconds per 1000 iterations with EWS of Dec α 500 MHz CPU.

SENSITIVITY STUDY

In the investigations for simulating the thermal behavior of a beam exposed to a localized fire ,S. Welch and A. Ptchlintsev has examined the influence of different grid resolutions , use of the WSGG radiation model and different numbers of rays in the discrete transfer model.

TABLE1 Test Conditions

Burner Size D (m)	Heat Release Rate Q (kW)	Distance H_B(m)	Q*
0.5	100	1	0.51
	150	1	0.76
	200	1	1.01
	95	0.6	0.48
	130	0.6	0.66
	160	0.6	0.81

As a result of their study, examination of the distribution of the temperature and total heat flux along the length of the beam showed that apart from the value in the stagnation point region, there was relatively little sensitivity to the variation of any of the model parameters over the rest of the range. However , when the number of ray vectors defined by θ and ϕ (see FIGURE. 3) was changed , it was evident that the analytical accuracy was improved as the number of rays increased. The number of ray vectors decide the location where the total radiation (radiation + reradiation) extend to . Therefore, we examined the influence of different numbers of rays, in our calculation. As for the number of ray vectors, ϕ was fixed at 8 while only θ was changed to 2, 4, and 8. The experimental data used for comparison were values of steady -state. The conditions of all the experiments are shown in Table 1 . In this study, we compared about the experimental conditions of the heat release rates Q= 100,150, and 200 (kW), and the height between the burner surface and the bottom of the beam(H_B)= 1(m).

RESULTS AND DISCUSSION

SENSITIVITY STUDY

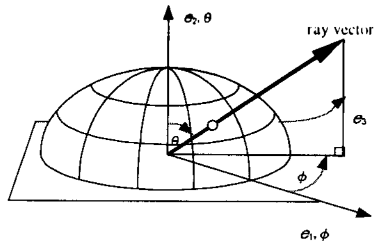

FIGURE. 3 Number of ray vectors defined by θ and ϕ

FIGURES.4～7show comparison between the predicted and experimental values of heat flux and temperature distribution on the lower flange and web with Q=100(kW),H_B=1(m). In the case of 32 divisions ,the predicted heat flux and temperature distribution are considerably lower than the experimental values. The maximum error of heat flux to the lower flange at the stagnation point is 16 (kW/m^2). In the case of 64 rays, the maximum errors of heat flux to the lower flange is about 7 (kW/m^2) at a point 0.3(m) from the stagnation point. The analytical results of the temperature distribution on the lower flange and web surface agreed well with the experimental values.

FIGURES.8～11 shows the analytical results and experimental values concerning the heat flux and temperature distribution on the lower flange and web with Q=150 (kW),H_B=1(m). In these FIGURES, the black-triangle points represent the calculation results of 16 rays and the white-triangle points show 32 rays. For both cases, the predicted result of the heat flux and temperature of the lower flange was higher than the experimental values at near from the stagnation point , with the difference being 17 (kW/m^2) and 80℃ for 16 divisions and 14 (kW/m^2) and 70℃ for 32 rays. As for the heat flux and temperature distribution of the web surface, the analytical results roughly agreed with the experimental values. The calculation results and measured values of heat flux distribution to the lower flange with Q=200 (kW) and H_B=1(m) are shown in FIGURE 12. In this figure, the number of ray vectors are changed 16, 32, and 64. From this graph , we can know that the analytical result with Q=200 (kW) and

H_B=1(m) did not show substantial deterioration of analytical accuracy, according to the number of rays, and it agreed fairly well with the experimental values. It is different from the case with Q=100 (kW) and H_B=1(m). As a whole, the calculated heat flux indicated lower than the experimental values for all points except for the stagnation point. When compared in terms of the number of rays, the errors of heat flux to near from the stagnation point is larger with decreasing number of ray vectors.

FIGURE.13 shows a comparison in terms of the distribution of heat flux to the web surface when Q =200 (kW) and H_B =1(m). The analytical results for heat flux agrees roughly well with the experimental values and they are less affected by the number of ray vectors. As described above, it should be noted that analytical accuracy may deteriorate greatly unless a large number of rays are set under analytical conditions with the heat generation rate as small as Q = 100 (kW). Since the difference between cases with 32 and 64 rays is small, however, the analytical result with a total of 32 rays(θ =4 and ϕ =8)was used subsequently for comparison between analytical results and experimental values in order to shorten the calculation time.

COMPARISON OF CALCULATIONS AND EXPERIMENTAL RESULTS

In this study ,data of experiments and predictions are compared at steady state. FIGURES. 14 and 15 show temperature distribution along the beam when Q =200 (kW) and H_B =1(m). The analytical results and experimental values agree comparatively well in both the lower flange and web. As for the lower flange, except the stagnation point, the region near from the stagnation point (r=0.9m) , the temperature of the lower flange were higher than other region, with the difference being a maximum of 100(℃). FIGURES.16 through 19 show the temperature and heat flux distribution with Q=95 (kW). FIGURES. 20 through 23 show the same comparison with Q=130 (kW), while FIGURES.24 through 27 show the same comparison with Q =160 (kW). In all cases, H_B was 0.6 (m). During analysis, calculation was made under conditions completely similar to the case in which H_B was 1.0 (m). When compared with the analytical result with H_B=1.0 (m), that with H_B = 0.6(m) showed large difference from the experimental values. With H_B = 0.6 m, the calculated results of heat flux were lower than experimental values regardless of the heat release rate. A large difference was observed within a distance of 0.6(m)from the stagnation point. Under experimental condition of Q= 130 (kW), the difference for the lower flange was a maximum of 18 (kW/m^2) at a point 0.15(m) from the stagnation point. In all experimental condition of H_B=0.6 (m) , the temperature decrease along the axial direction is more slowly in the analytical results than in experimental values.

The experiment have shown that the heat flux to the downward surface of the lower flange was controlled primarily by the flame length which flows along the lower surface of the beam [1]. The flame length can be represented as a function of Q^*_{DHB}.

$$Q^*_{DHB} \equiv Q / \rho C_P T_0 g^{1/2} DH_B^{3/2} \quad \cdots (5)$$

As is known from the experiment that the increase of the flame length becomes insignificant as (Q^*_{DHB}) is increased in the domain of (Q^*_{DHB})>0.35, and the increase of flame length with the increase in the heat release rate Q was not remarkable in the case of H_B=0.6(m). This was different from the case with H_B=1.0(m). The difference of the analytical accuracy is depending on the height between the burner surface and bottom of the beam(H_B) . It may be attributed

mainly to the failure to show the above actual phenomenon in the analytical model.

FIGURES.28 shows the relationship between analytical error of heat flux and the dimensionless heat release rate (Q^*_{DHB}) , assuming a characteristic length-scale (H_B).

Also FIGURE.29 shows the relationship between analytical error of the temperature and Q^*_{DHB}. In FIGURE.28, values on the main axis indicate the maximum difference between analytical and experimental values .That on the second axis (a right vertical axis) indicate the ratio of error for the maximum heat flux measured in each experiment. Comparison of values on the main axis of the figure shows that the error for heat flux increases with increasing Q^*_{DHB} for both lower flange and web. In the case of the lower flange, the error for heat flux is larger under three experimental conditions (Q^*_{DHB} ranging from 0.35 to 0.5), with H_B being 0.6m than under conditions with H_B being 1m. In this case ,the maximum difference is 22 (kW/m^2).

CONCLUSIONS

We have conducted the prediction of the thermal response of a steel beam installed beneath a ceiling and exposed to a localized fire source by using CFD model. From the results of the calculation, following conclusions can be drawn.

(1) The number of ray vectors was changed to 16, 32, and 64 and the effects on analytical results were compared. The analytical results for heat flux with 32 ray vectors under experimental conditions with Q = 100 (kW) and H_B =1(m) was considerably lower, with the difference from the experimental values at the stagnation point being a maximum of 80%. Under conditions with 64 ray vectors or a higher heat release rate, the analytical results agreed well with the experimental values concerning heat flux distribution. It is known from this fact that , in the case of the lower heat release rate ,the analytical accuracy may deteriorate substantially unless the number of ray vectors is increased.

(2) Under any conditions of H_B=0.6(m), the analytical results for heat flux was lower than the experimental values. Under experimental conditions with a heat release rate of 160(kW), the difference was 27 (kW/m^2),which is equivalent to about 47% of the maximum heat flux in the experiment.

(3) Concerning the heat flux, the error increased with increasing Q^*_{DHB}. In the case of the lower flange, the error for heat flux is larger under three experimental conditions with H_B =0.6m (Q^*_{DHB} ranging from 0.35 to 0.5)than under conditions with H_B=1m. In this case ,the maximum difference is 22 (kW/m^2). While the error for the heat flux scattered within 20% to 56% of the maximum heat flux measured in the experiment, the maximum error for the temperature remained 22%.

The analytical accuracy differed considerably when experimental condition of H_B=0.6 (m) were calculated using same analytical conditions tuned for H_B=1.0(m). In the case of H_B=1.0(m), prediction is possible with a practical accuracy. When the distance between the burner surface and the bottom of the beam(H_B) is varied, however, it will be necessary to tune calculation conditions again.

Systematic studies will be made on how to set the calculation conditions for any combination of distance(H_B) and the heat release rates(Q). It is necessary to identify the cause for analytical error encountered in this study.

ACKNOWLEDGMENTS

The authors wish to thank assistant Prof., Sinsuke Kato of Tokyo Univ. and Dr.Ryuichiro Yoshie of Maeda Corporation for the advice of numerical simulation using CFD model. The authors are also indebted to Mr. Y.Yokobayashi, Sekisui House Ltd., for the assistance in the experiments .

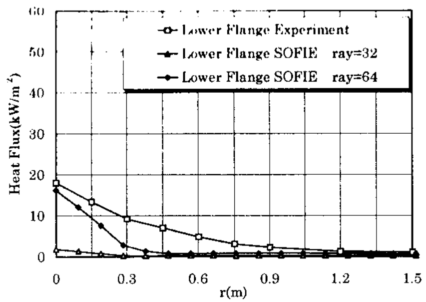

FIGURE.4 Effects of the Number of Ray Vector Q=100(kW), H_B =1.0(m)

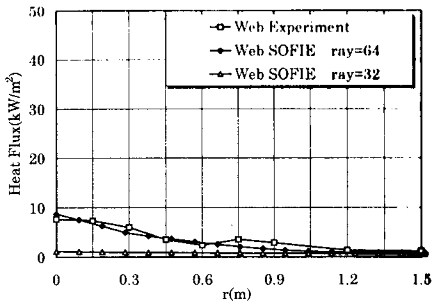

FIGURE.5 Effects of the Number of Ray Vector Q=100(kW), H_B =1.0(m)

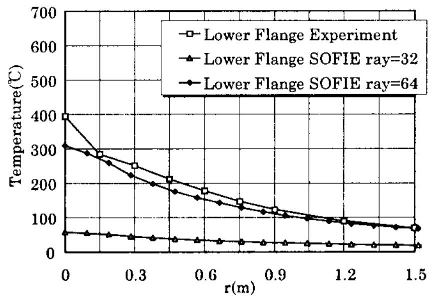

FIGURE.6 Effects of the Number of Ray Vector Q=100(kW), H_B =1.0(m)

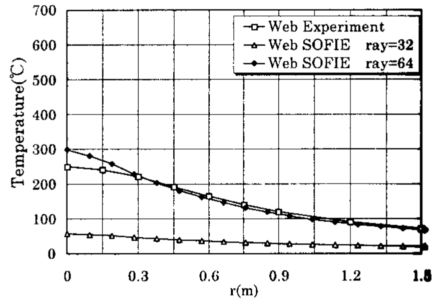

FIGURE.7 Effects of the Number of Ray Vector Q=100(kW), H_B =1.0(m)

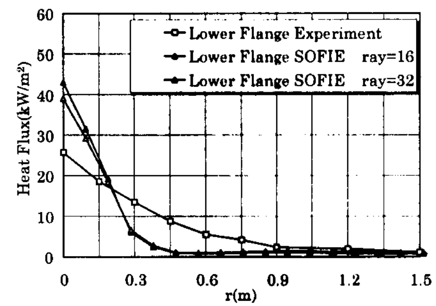

FIGURE.8 Effects of the Number of Ray Vector Q=150(kW), H_B =1.0(m)

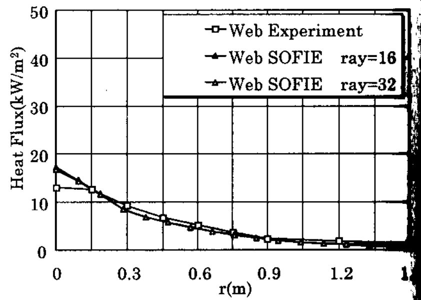

FIGURE.9 Effects of the Number of Ray Vector Q=150(kW), H_B =1.0(m)

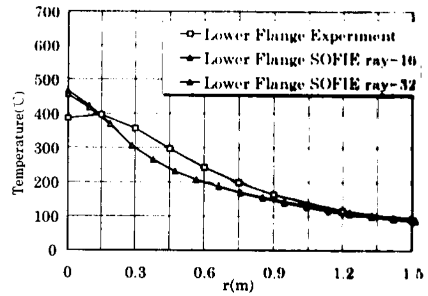

FIGURE.10 Effects of the Number of Ray Vector Q=150(kW), H_B =1.0(m)

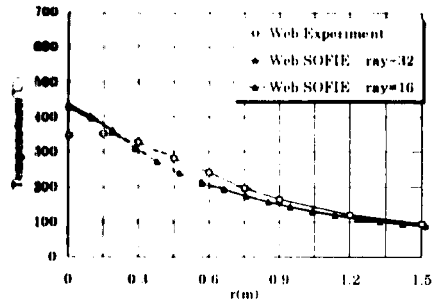

FIGURE.11 Effects of the Number of Ray Vector Q=150(kW), H_B =1.0(m)

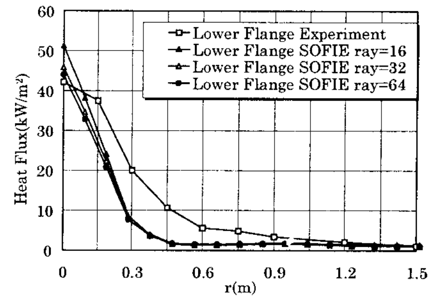

FIGURE.12 Effects of the Number of Ray Vector Q=200(kW), H_B =1.0(m)

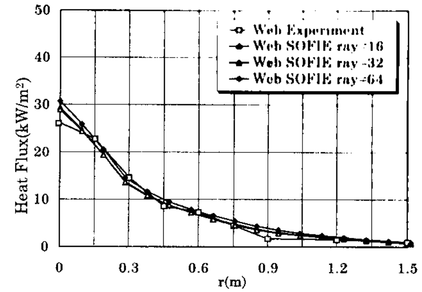

FIGURE.13 Effects of the Number of Ray Vector Q=200(kW), H_B =1.0(m)

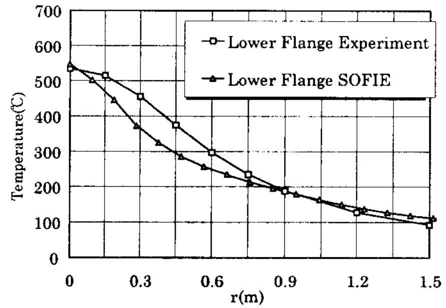

FIGURE.14 Temperature distribution (lower flange) Q=200(kW), H_B =1.0(m)

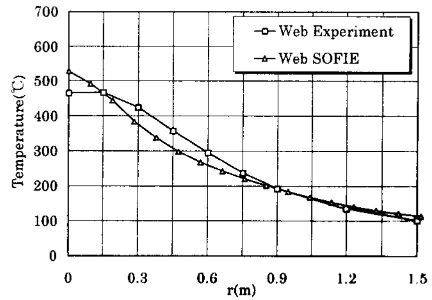

FIGURE.15 Temperature distribution (web) Q=200(kW), H_B =1.0(m)

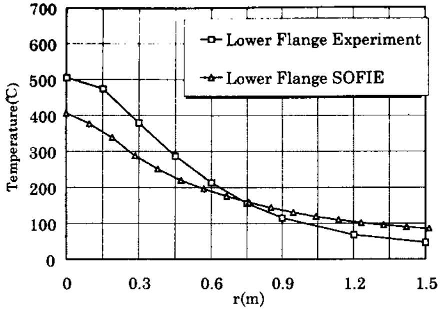

FIGURE.16 Temperature distribution
(lower flange) Q=95(kW), H_B =0.6(m)

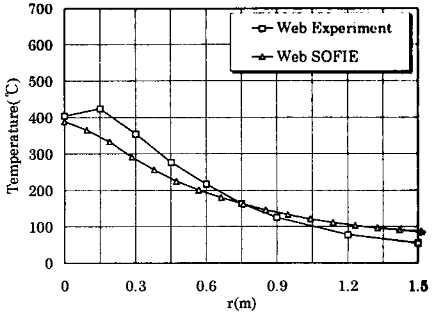

FIGURE.17 Temperature distribution
(web) Q=95(kW), H_B =0.6(m)

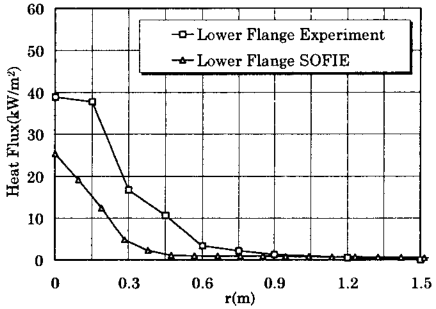

FIGURE.18 Heat flux distribution
(lower flange) Q=95(kW), H_B =0.6(m)

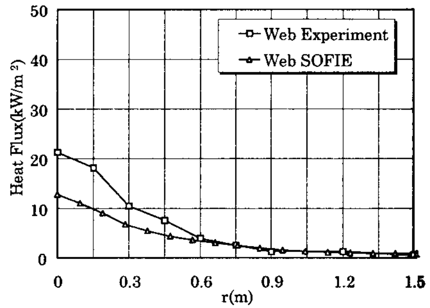

FIGURE.19 Heat flux distribution
(web) Q=95(kW), H_B =0.6(m)

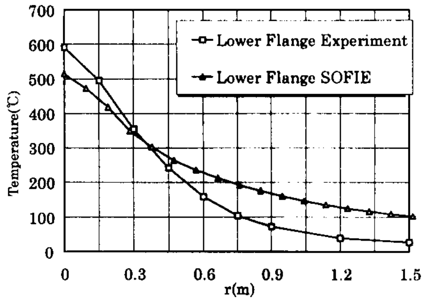

FIGURE.20 Temperature distribution
(lower flange) Q=130(kW), H_B =0.6(m)

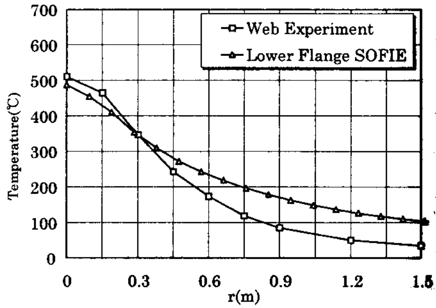

FIGURE.21 Temperature distribution
(web) Q=130(kW), H_B =0.6(m)

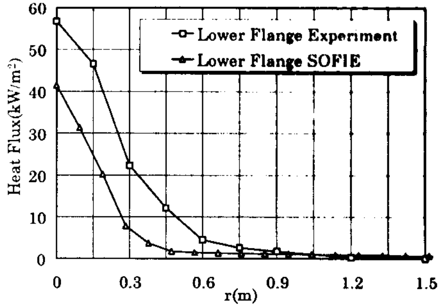

FIGURE.22 Heat flux distribution
(lower flange) Q=130(kW), H_B =0.6(m)

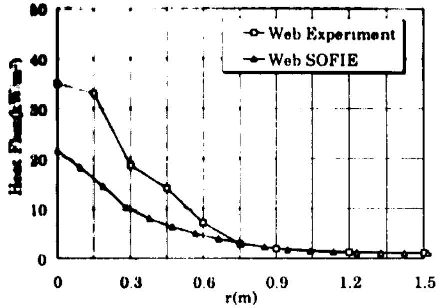

FIGURE.23 Heat flux distribution
(web) Q=130(kW), H_B =0.6(m)

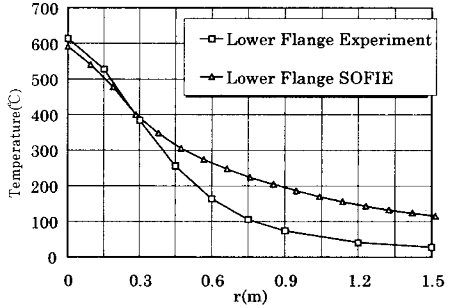

FIGURE.24 Temperature distribution
(lower flange) Q=160(kW), H_B =0.6(m)

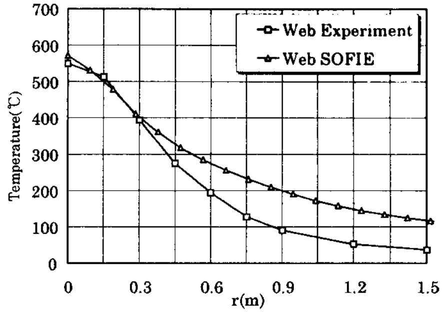

FIGURE.25 Temperature distribution
(web) Q=160(kW), H_B =0.6(m)

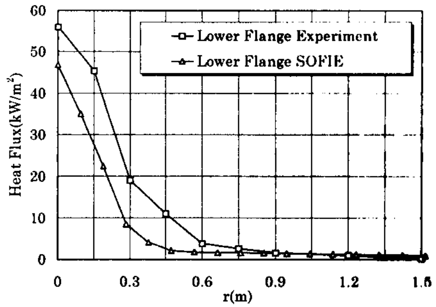

FIGURE.26 Heat flux distribution
(lower flange) Q=160(kW), H_B =0.6(m)

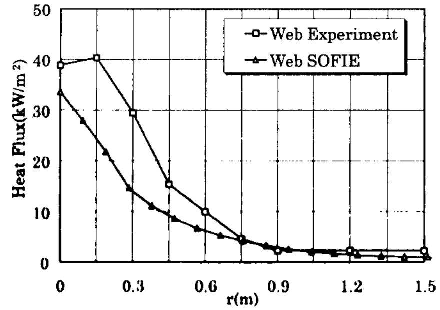

FIGURE.27 Heat flux distribution
(web) Q=160(kW), H_B =0.6(m)

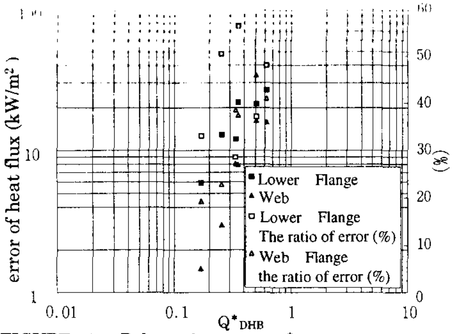

FIGURE.28 Relation between Q^*_{DHB} and error of heat flux.

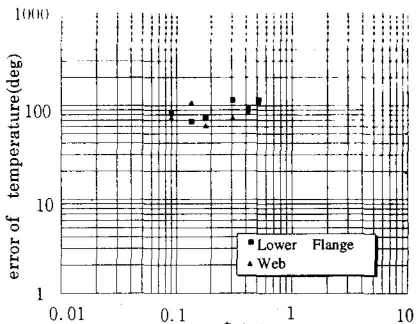

FIGURE.29 Relation between Q_{HB}* and error of temperature.

REFERENCE

1) Yokobayashi,Y.,Hasemi,Y.,Wakamatsu, T., Wakamatsu, T., "Experimental Study on the Heating Mechanism and Thermal Response of a Steel Beam Under Ceiling Exposed to a Localized Fires ," Journal of Structural and Construction Engineering, Transactions of AJI , No .498 (in Japanese)
2) Wakamatsu,T.,Hasemi,Y., Yokobayashi, Y.,A.V.Ptchelintsev,"Heating Mechanism of Building Components Exposed to a Localized Fire - FEM Thermal and Structural Analysis of a Steel Beam Under Ceiling," Proceedings, OMAE '97 Yokohama 1997
3) Wakamatsu, T.,Hasemi, Y., "Heating Mechanism of Building Components Exposed to a Localized Fire- FDM Thermal Analysis of a Steel Beam Under Ceiling -," Fire Science and Technology - Proceedings of the Third Asia-Oceania Symposium, Singapore pp335-346,1998.06
4) Hara, T., Yokoi, M., Morikawa, Y., " Analysis of Thermal Plumes with Numerical Simulation and Experimental Results Basic Plume Analyses for the CFD Performance of the Standard k-e model. Annual Meeting," Architectural Institute of Japan , 1998(in Japanese)
5) Yoshie, R.,WEI Ran, " CFD Analysis of Fire Plume - (Part1) Influence of Computational Domain and Mesh Division on Numerical solution," Annual Meeting, Architectural Institute of Japan , 1998(in Japanese)
6) Yoshie,R. ,and WEI Ran "CFD Analysis of Fire Plume - (Part2) Influence of Numerical scheme for convection terms and model for fire source," Annual Meeting, Architectural Institute of Japan , 1998(in Japanese)
7) Welch, S.,P.Rubini "SOFIE Users Manual" School of Mechanical Engineering, Cranfield University, 1996
8) A.V.Ptchelintsev, M.Nikolaenko, Hayashi, Y., Wakamatsu, T. ,"Sofie Computation of the BRI Room Corner Fire Interim Report", SOFIE meeting, 1998
9) Rodi, W. "Turbulent buoyant jets and plumes", Pergamon, 1982
10) Bressloff, N.W., Moss, J.B., Rubini, P.A."Assessment of a differential total absorptivity solution to the radiative transfer equation as applied in the discrete transfer radiation model", Numerical Heat Transfer, Part B: Fundamentals, vol. 29, part 3, pp. 381-397, May, 1996
11) Bressloff, N.W., Moss, J.B., Rubini, P.A. "CFD prediction of coupled radiation heat transfer and soot production in turbulent flames," Twenty-sixth Symposium on Combustion, The Combustion Institute, pp. 2379-2386, 1996
12) "Fire safety design method, comprehensive fire preventing procedures, ed. by Japan Institute of Construction Engineering," vol.4, April, 1988 (in Japanese)
13) S.Welch,A.Ptchelintsev., "Numerical Prediction of Heat Transfer to a Steel Beam in a Localized Fire," Proceedings of the Second International SeminarFire-and Explosion Hazard of Substances and Venting of Deflagrations,11-15 August, 1997, Moscow, Russia, pp. 299-313.

Fires in Tunnels: Three-Dimensional Numerical Simulation and Comparison with the Experiment

ALEXEY V. KARPOV, DMITRY V. MAKAROV, VLADIMIR V MOLKOV and ALEXEY M. RYZHOV
All-Russian Research Institute for Fire Protection,
VNIIPO 12, Balashikha-3, Moscow region, 143900 Russia

ABSTRACT

The computational fluid dynamics code SOFIE has been used for three-dimensional unsteady simulation of experimental fire in the tunnel with sizes 21x1.5x1.6 m performed previously by Japanese researchers. The steady and unsteady burning rate approaches were used for numerical modeling. It has been shown that the computed flow velocities and temperature distribution for unsteady, growing in time, burning rate are in better correspondence to the experimental data. It is shown that an approach to the description of burning rate influences significantly on the magnitude and the distribution of heat fluxes in the enclosure, that is important in particular for solving the fire resistance problem.

KEYWORDS

Fire, tunnel, unsteady CFD modelling, variable burning rate, temperature, velosity, heat flux

INTRODUCTION

The computational fluid dynamics (CFD) is employed more and more often for fire phenomena investigation during last decades. CFD modeling is the essential tool for performance based approach to fire safety engineering. It enables to realize reliable cost-effective fire safety design of the premises, minimize expenses on testing, study regularities of fire phenomena in numerical experiments.

The CFD technique of fire modeling is the most informative because it calculates time and space distribution of thermo- and hydrodynamic parameters. Advanced CFD codes become more complicated and take into account new physical aspects of fire phenomenon. On the one hand it gives new parameters which being varied can influence on numerical solution. On the